Thin Solid Films 557 (2014) 197–202

Contents lists available at ScienceDirect

Thin Solid Films

journal homepage: www.elsevier.com/locate/tsf

Conductive and transparent V-doped ZnO thin films grown by radio frequency magnetron sputtering

Shuhei Okuda *, Takuya Matsuo, Hiroshi Chiba, Tatsuya Mori, Katsuyoshi Washio

Graduate School of Engineering, Tohoku University, Sendai 980-8579, Miyagi, Japan

ARTICLE INFO

Available online 17 January 2014

Keywords:
Transparent conducting oxide
ZnO
Transition metal
Vanadium
Radio frequency magnetron sputtering

ABSTRACT

Transparent conductive films of vanadium (V)-doped zinc oxide (VZO) were deposited by radio frequency magnetron sputtering on quartz substrates using a ceramic ZnO target with V chips. The electric, optical and structural properties of VZO thin films (V concentration of 0–4 at.%) were investigated at various substrate temperatures (T_{SUB}) from 200 to 600 °C. The resistivity sharply decreased by V doping, and the resistivity reached a minimum of about 5×10^{-4} Ωcm and 1×10^{-3} Ωcm for $T_{SUB} = 200$ °C and 600 °C, respectively. It was almost constant up to V concentration of 1.0–1.5% and gradually increased at higher V concentration. The optical transmittance ($\lambda = 500$ nm) of VZO films (V = 0.9–1.1%) drastically degraded from about 80% to 40% for T_{SUB} of below 225 °C while that of ZnO films was over 83% for T_{SUB} of over 200 °C. From the dependence of growth rate and the expansion of c-axis lattice constant in the VZO film, the V configuration was considered to have a charge number of 3.

1. Introduction

Transparent conductive oxides (TCOs) have been considered as an essential material for many optoelectronic devices such as flat panel displays. Indium tin oxide (ITO) is currently the most widely-used material for transparent electrodes due to an advantage in terms of electrical and optical properties [1,2]. However, a stable supply of ITO is difficult because of the cost and scarcity of indium. Therefore, impurity-doped zinc oxide (ZnO) has been extensively studied as an alternative to ITO in recent years [3–6]. ZnO has a wide bandgap of about 3.3 eV at room temperature, and it is transparent to visible light. Low resistivity on the order of 10^{-5} Ωcm was obtained in the case of aluminum-doped ZnO [1,7]. Doping of transition-metal ions [8], which have a potential to take a wide variety of both valence binding configurations and coordination numbers, enables us to achieve low-resistivity and high-optical transmittance characteristics, ferromagnetic property, and piezoelectricity [9–16]. In this paper, the transition metal vanadium (V) was selected as the dopant, and the effects of the substrate temperature and V concentration on characteristics of V-doped ZnO thin films (VZO) were investigated.

2. Experiment

VZO thin films (500 nm thick) were deposited on quartz substrates by radio frequency magnetron sputtering. The gas used during the deposition was Ar (1.0 Pa). Sputtering conditions of radio frequency power and the substrate temperatures (T_{SUB}) were 150 W and 150–600 °C, respectively. V was doped by co-sputtering a ceramic ZnO with V chips. V concentration was measured by X-ray fluorescence (Rigaku RIX2100 using Rh radiation). The c-axis crystalline orientation was evaluated by out-of-plane X-ray diffraction (XRD, Rigaku SmartLab using CuKα radiation). The X-ray source was operated at a power of 40 kV × 30 mA. The cross-sectional structures were observed by transmission electron microscopy (TEM, Hitachi HF-2000 operated at 200 kV). All samples were prepared through thinning by using grinder and ion-milling. The surface morphology was observed by atomic force microscope (AFM, Park XE-100, using non-contact mode). Electrical properties were evaluated by four-point probe measurement (resistivity) and Hall effect measurement (resistivity, carrier density and mobility). Optical transmittance was measured by using an ultraviolet-near infrared ray spectrophotometer in the range from 300 to 1100 nm.

3. Results and discussion

3.1. Deposition

V concentration was proportionally controlled by V chip count, as shown in Fig. 1. V concentration at $T_{SUB} = 600$ °C was slightly higher than that at $T_{SUB} = 200$ °C for the same V chip counts. The dependence

* Corresponding author. Tel.: +81 22 263 7122; fax: +81 22 263 9396.
E-mail address: okuda@ecei.tohoku.ac.jp (S. Okuda).

0040-6090/$ – see front matter © 2014 Elsevier B.V. All rights reserved.
http://dx.doi.org/10.1016/j.tsf.2014.01.027

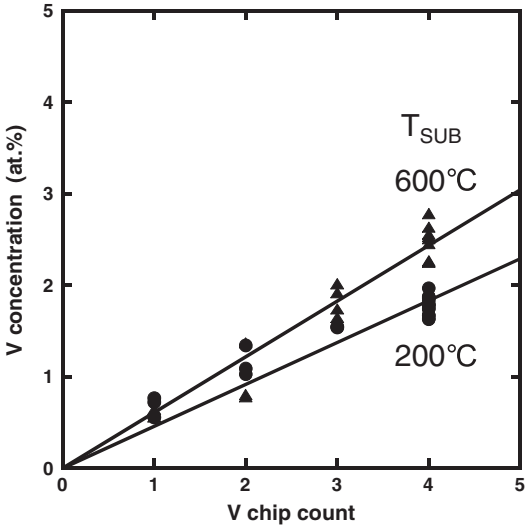

Fig. 1. Dependence of V concentration on V chip count in VZO films for T_{SUB} = 200 and 600 °C.

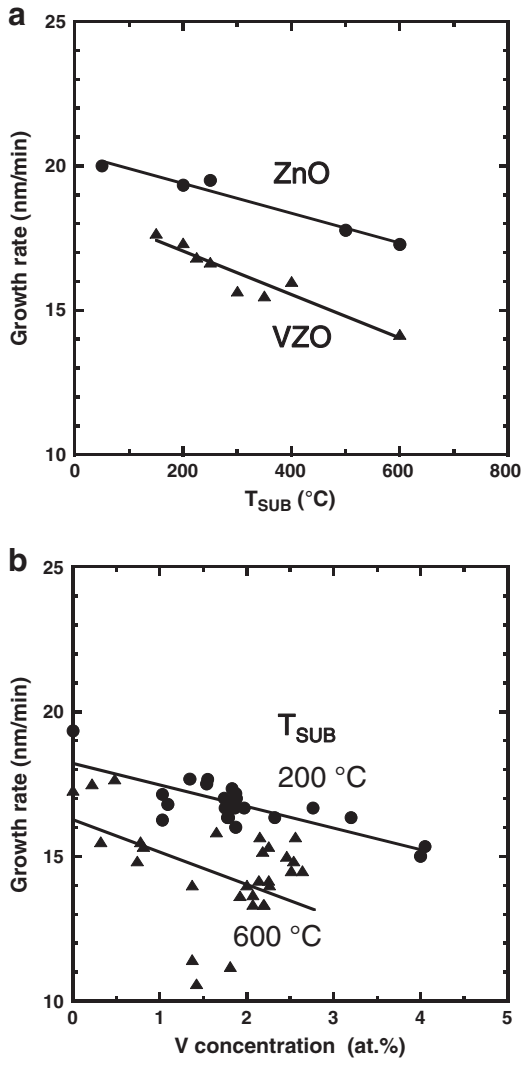

Fig. 2. (a) Dependence of growth rate of ZnO and VZO (V = 0.9–1.1 at.%) films on T_{SUB}. (b) Dependence of growth rate on V concentration in VZO films for T_{SUB} = 200 and 600 °C.

of growth rate of ZnO and VZO (V = 0.9–1.1 at.%) films on T_{SUB} is shown in Fig. 2 (a). The growth rate of ZnO and VZO decreased with increasing T_{SUB}, and the decrease ratio of VZO growth rate is higher than that of ZnO. The dependence of the growth rate on V concentration in VZO films for T_{SUB} = 200 and 600 °C is shown in Fig. 2 (b). The growth rate of VZO decreased with increasing V concentration, and its decrease ratio was higher for T_{SUB} = 600 °C though having large dispersion.

3.2. Crystalline structure

The XRD patterns of ZnO and VZO films are shown in Fig. 3. In the case of T_{SUB} = 200 °C (Fig. 3 (a)), the diffraction peaks from (002), (101), (102), (103) and (004) planes were observed in ZnO films. The diffraction peaks from (002) and (004) planes became weak gradually with increasing V concentration in VZO films. This means the c-axis crystalline orientation was deteriorated by V doping. Furthermore, the diffraction peaks from (101) became also very weak in VZO films of over 1.5-at.% V concentration.

In the case of T_{SUB} = 600 °C (Fig. 3 (b)), intense peaks from (002) and (004) planes were observed compared to T_{SUB} = 200 °C. This

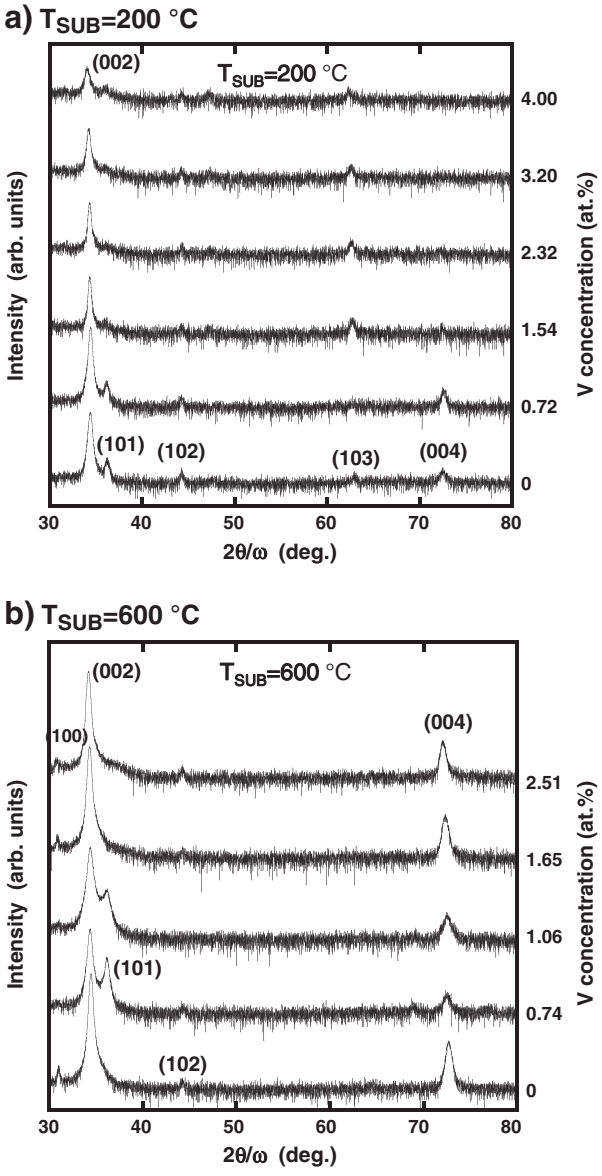

Fig. 3. XRD patterns of ZnO and VZO films at (a) T_{SUB} = 200 °C and (b) 600 °C with various V concentrations.

indicates that c-axis orientation improved at high T_{SUB}. The distinctive feature is observed for V doping of 0.74 and 1.06 at.%. That is, the peak from (101) was observed, the peaks from (002) and (004) plane weakened, and the peak from (100) plane disappeared. The dependence of XRD (002) diffraction intensity on V concentration for T_{SUB} = 200 °C and 600 °C is shown in Fig. 4. As described in the explanation of Fig. 3, an anomalous zone of V concentration (shaded area) indicating peculiar dependence was confirmed. That is, the intensity for T_{SUB} = 600 °C decreased and that for T_{SUB} = 200 °C increased, contrary to the over-all tendency (depicted by broken lines). The reason why this anomalous dependence was observed is not clear at this point. Because, there's no common feature in the change of XRD patterns on V doping concentration between T_{SUB} = 200 °C and T_{SUB} = 600 °C. In any case, there's an unstable transition region at about 1-at.% V concentration concerning the c-axis orientation. The dependence of c-axis lattice constant on V concentration at T_{SUB} = 200 °C and 600 °C is shown in Fig. 5. The c-axis lattice constant was estimated from the (002) diffraction angle. The c-axis lattice constant of crystal ZnO grown by the hydrothermal method is 5.206 Å. In this study, ZnO expanded slightly at T_{SUB} = 200 °C and shrank at T_{SUB} = 600 °C along the c-axis. There is a dispersion of about 0.015 Å but no particular dependence is observed up to about 1-at.% V doping for T_{SUB} = 200 °C. But besides that, the c-axis lattice constant of VZO increased proportionally to the V concentration. The cross-sectional TEM images of VZO (V = 1.7 at.%) and the selected area electron diffraction (SAED) patterns are shown in Fig. 6, for (a) T_{SUB} = 200 °C and (b) T_{SUB} = 600 °C. As predicted in XRD measurements, columnar grains perpendicular to the quartz substrate surface are confirmed for both T_{SUB}. As shown in enlarged images of the VZO/quartz interface, the columnar structure was seen immediately above the interface for T_{SUB} = 600 °C, while, a specific orientation was not observed near the interface for T_{SUB} = 200 °C. Therefore, the grain size of VZO is considered to be very small in the early stage of growth at T_{SUB} = 200 °C, and this deteriorates the c-axis orientation. As shown in the SAED diffraction pattern, the crystalline structure for T_{SUB} = 200 °C is disordered while it has a little order for T_{SUB} = 600 °C. The [0001] diffraction spot for T_{SUB} = 600 °C was more intense than that of T_{SUB} = 200 °C. These indicate that VZO grown at a high temperature was improved in the c-axis orientation, as seen in ZnO growth [17].

3.3. Morphology

The surface roughness caused by the columnar structure was observed from TEM images (Fig. 6). The dependence of surface roughness

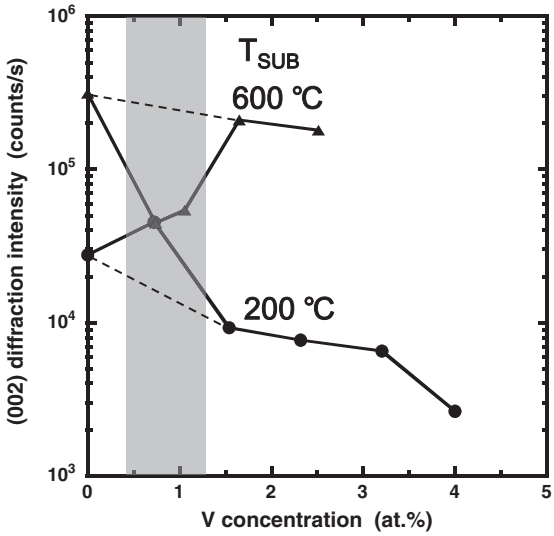

Fig. 4. Dependence of XRD (002) diffraction intensity of ZnO and VZO films at T_{SUB} = 200 °C and 600 °C on V concentration.

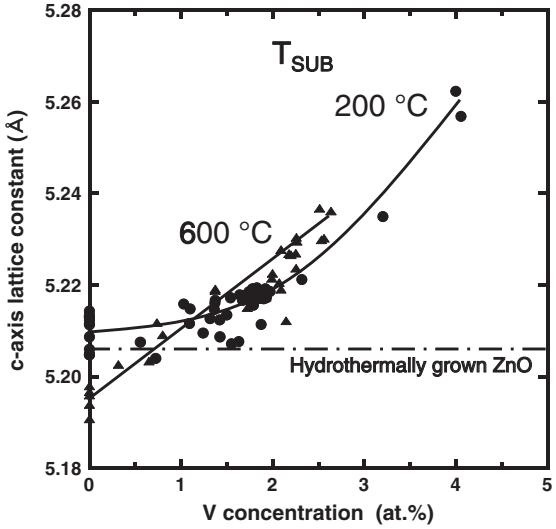

Fig. 5. Dependence of c-axis lattice constant of ZnO and VZO films at T_{SUB} = 200 °C and 600 °C on V concentration.

on T_{SUB} for ZnO and VZO films (V = 0.9–1.1 at.%) and AFM images are shown in Fig. 7. The surface roughness of ZnO at T_{SUB} = 200 °C was very large at about 9 nm and that at T_{SUB} = 600 °C reduced by half. On the other hand, the surface roughness of VZO increased slightly with T_{SUB} and it was in the range of 4–6 nm. The grain size of VZO was obviously smaller than that of ZnO. In the case of ZnO, the grain size at T_{SUB} = 600 °C was slightly smaller than that at T_{SUB} = 200 °C. This induced the surface roughness to decrease. However, in the case of VZO, small circular grains at T_{SUB} = 200 °C coalesced into snaky lines at T_{SUB} = 600 °C. Therefore, this resulted in an increase of surface roughness.

3.4. Resistivity and transmittance

The dependences of resistivity, carrier density, and Hall mobility on V concentration for VZO films grown at T_{SUB} = 200 °C and 600 °C are shown in Fig. 8. The resistivity decreased sharply by V doping. It was almost constant up to a V concentration of 1.0–1.5 at.% and increased gradually with increasing V concentration. The lowest resistivity was 5.0×10^{-4} Ωcm and 1.2×10^{-3} Ωcm, for T_{SUB} = 200 °C and 600 °C, respectively. The carrier density of VZO films was in the range of between 10^{20} and 10^{21} cm^{-3} by V doping and the averaged carrier density for T_{SUB} = 200 °C was about twice that for T_{SUB} = 600 °C. The carrier density was almost constant for T_{SUB} = 200 °C while it decreased with increasing V doping for T_{SUB} = 600 °C. The maximum Hall mobility for T_{SUB} = 200 °C was about twice that for T_{SUB} = 600 °C for V concentration of about 1 at.%. This is the main reason that caused the difference of minimum resistivity. The Hall mobility for T_{SUB} = 200 °C decreased with increasing V concentration while it was almost constant for T_{SUB} = 600 °C. The dependences of resistivity, carrier density and Hall mobility on T_{SUB} for VZO films (V = 0.9–1.1 at.%) are shown in Fig. 9. The resistivity increased with T_{SUB} over 400 °C. In contrast, the carrier density decreased for T_{SUB} over 400 °C. The Hall mobility decreased with increasing T_{SUB} over 200 °C. As a result, the minimum resistivity was obtained for T_{SUB} = 200 °C. The dependences of the resistivity and the optical transmittance at wavelength of 500 nm on T_{SUB} for both ZnO and VZO films (V = 0.9–1.1 at.%) were shown in Fig. 10. The resistivity of 6.3×10^{-4} Ωcm with the optical transmittance of 78% was obtained at the substrate temperature of 250 °C. This is the most appropriate condition to apply VZO films as TCO films at this point. The optical transmittance of ZnO film was over 83% for T_{SUB} of over 200 °C, however, that of VZO film was drastically degraded for T_{SUB} of below 225 °C. The transmittance spectrum of VZO

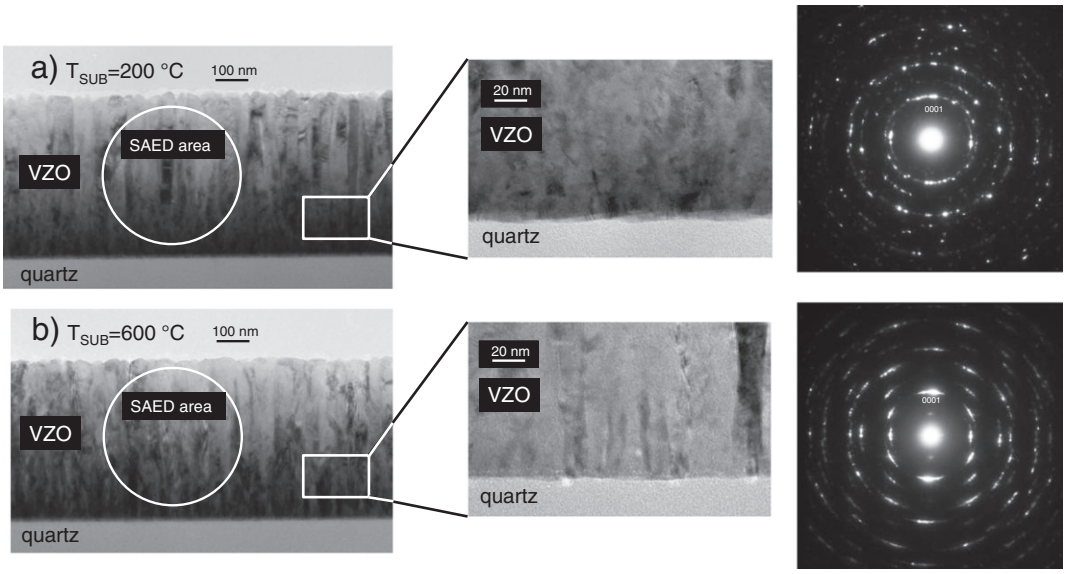

Fig. 6. Cross-sectional TEM images and selected area electron diffraction (SAED) patterns of VZO (V = 1.7 at.%) films for (a) T_{SUB} = 200 °C and (b) 600 °C.

films (V = 0.9–1.1 at.%) for T_{SUB} = 200, 225 and 250 °C were shown in Fig. 11. Even though the change of T_{SUB} was only 25 °C, the optical transmittance for T_{SUB} = 225 °C is about half of that for T_{SUB} = 200 °C.

4. Discussion

The ionization energy of Zn^{2+} is 17.96 eV, while those of V^{2+} and V^{3+} are 14.65 and 29.31 eV, respectively [18]. Therefore, to explain high V concentration at high T_{SUB} (Fig. 1) and the decrease of growth rate of VZO (Fig. 2), it should be considered that the charge number of V is probably +3. This is because a high ionization energy must be provided to dope V into ZnO. The decrease ratio of growth rate at high T_{SUB} in VZO is also explained by this V configuration. The reason why V^{3+} ions incorporate into the wurtzite ZnO structure despite the coordination number of 6 is not clear. But, considering that the growth rate of VZO decreased with increasing V concentration, as shown in Fig. 2 (b), this speculation brings good coincidence of the observed phenomena.

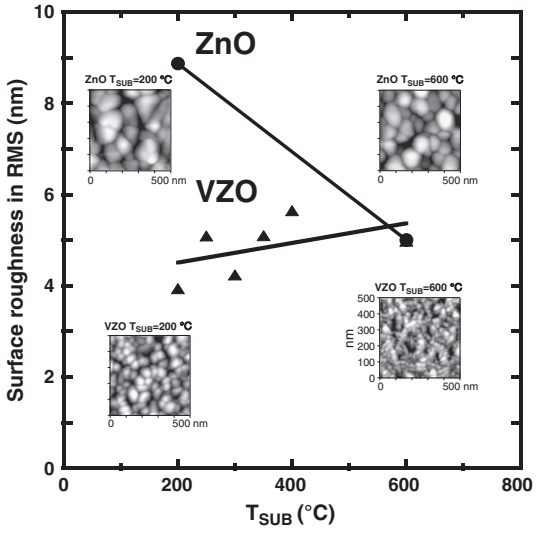

Fig. 7. Dependence of surface roughness on T_{SUB} for ZnO and VZO films (V = 0.9–1.1 at.%) with AFM images.

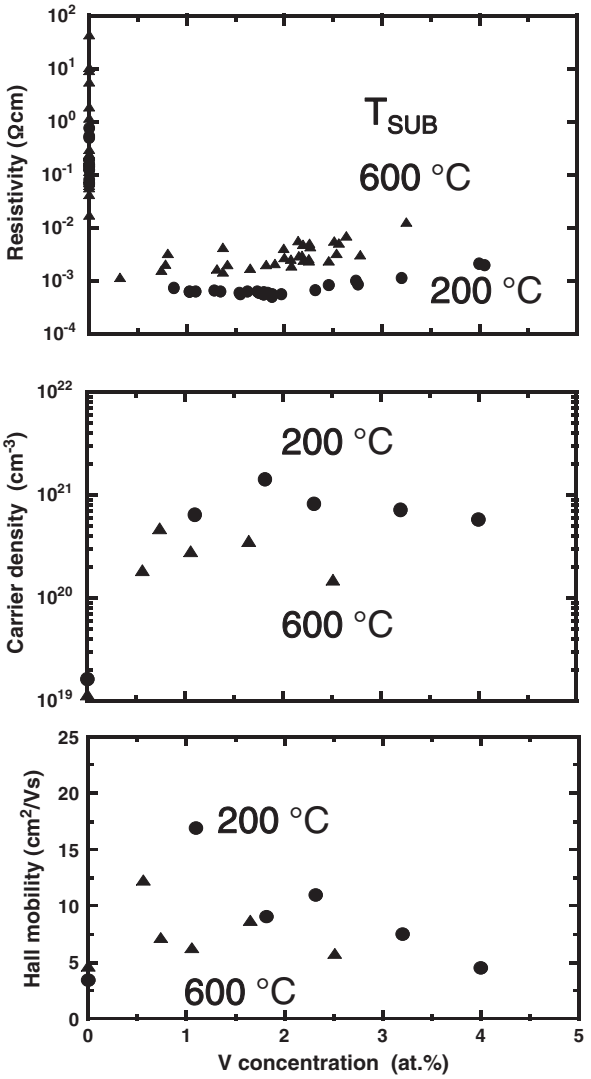

Fig. 8. Dependences of resistivity, carrier density, and Hall mobility on V concentration for VZO films grown at T_{SUB} = 200 °C and 600 °C.

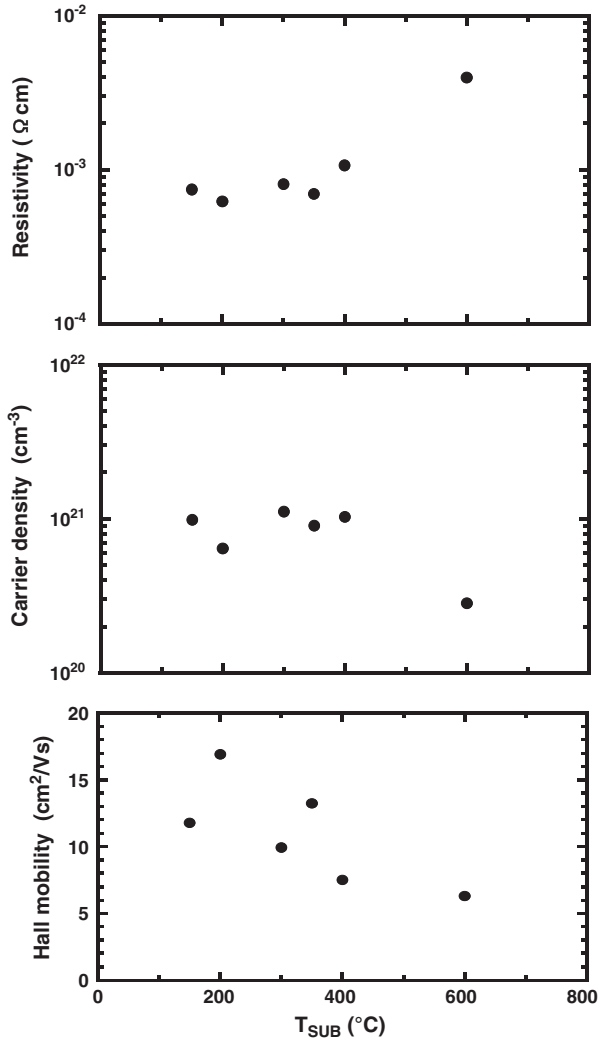

Fig. 9. Dependence of resistivity, carrier density and Hall mobility on T_{SUB} for VZO films (V = 0.9–1.1 at.%).

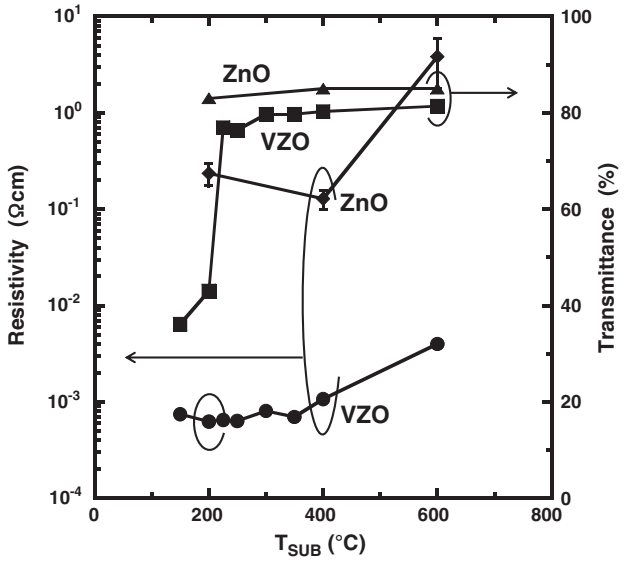

Fig. 10. Resistivity and optical transmittance at wavelength of 500 nm on T_{SUB} for both ZnO and VZO films (V = 0.9–1.1 at.%).

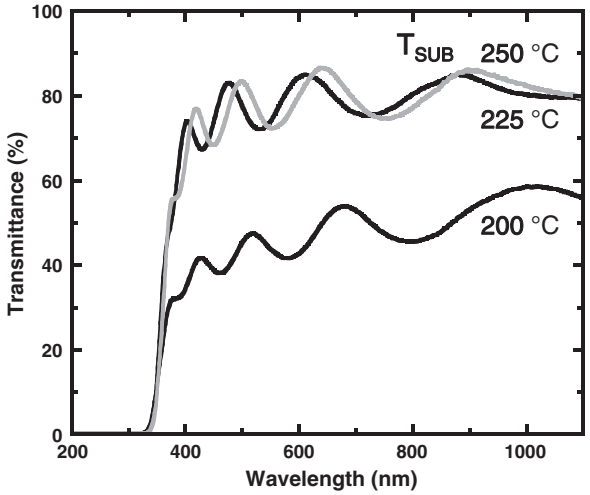

Fig. 11. Transmittance spectrum of VZO films (V = 0.9–1.1 at.%) for T_{SUB} = 200, 225 and 250 °C.

The above-mentioned V^{3+} incorporation is also supported by the expansion of c-axis lattice constant in VZO (Fig. 5). The ionic radius of V^{3+} is 0.64 Å and is about 10% longer than that of Zn^{2+} (0.6 Å). In addition, resistivity of vanadium oxide V_2O_3 is about 10^{-4} Ωcm while that of V_2O_5 is about 10^2 to 10^3 Ωcm at room temperature [19,20]. This supports the V charge number of +3 because the resistivity of VZO films is down to 10^{-3} Ωcm. Furthermore, the increment of carrier density is well accorded with V concentration. We've tried to obtain the verification of V charge number of 3. However, through Raman scattering, photoluminescence, and X-ray photoelectron spectroscopy, the evidence was not so strong that we could actually confirm it. This is because the amount of V is too small to get data. Therefore, the charge number of 3 remains a matter of speculation at this point. We'd like to make continuous efforts to provide further confirmation. That is, this means that V atoms located at the substitutional site are univalent. The reason why the carrier density and Hall mobility of VZO decreased with increasing V over 2 at.% is considered to be caused by the formation of V–V clusters or V_xO_y oxides.

The reason causing the drastic degradation of optical transmittance in VZO films between T_{SUB} = 200 and 225 °C is not clear. This is because it is well-known that the high carrier density causes the deterioration of the optical transmittance but the carrier density for T_{SUB} = 200 and 225 °C is nearly the same.

5. Conclusion

The characteristics of VZO films deposited by radio frequency magnetron sputtering on quartz substrates have been investigated. As a result, there were some kinds incomprehensible phenomena, but relatively low resistivity and good optical transmittance were obtained for VZO of about 1-at.% V concentration.

Acknowledgment

This study was partially supported by The Industry-Academia Collaborative R&D Programs from The Japan Science and Technology Agency, and by JSPS Core-to-Core Program, A. Advanced Research Networks.

References

[1] T. Minami, Semicond. Sci. Technol. 20 (2005) S35.
[2] R.B.H. Tahar, T. Ban, Y. Ohya, Y. Takahashi, J. Appl. Phys. 83 (1998) 2631.
[3] X. Jiang, F.L. Wong, M.K. Fung, S.T. Lee, Appl. Phys. Lett. 83 (2003) 9.

[4] M. Lorenz, E.M. Kaidashev, H.V. Wenckstem, V. Riede, C. Bundesmann, D. Spemann, G. Benndorf, H. Hochmuth, A. Rahm, H.C. Semmelhack, M. Grundmann, Solid State Electron. 47 (2003) 2205.
[5] J. Jia, A. Takasaki, N. Oka, Y. Shigesato, J. Appl. Phys. 112 (2012) 013718.
[6] M. Lorenz, C. Schmidt, G. Benndort, T. Bontgen, H. Hochmuth, R. Bottcher, A. Poppl, D. Spemann, M. Grundmann, J. Phys. D. Appl. Phys. 46 (2013) 065311.
[7] H. Agura, A. Suzuki, T. Matsushita, T. Aoki, M. Okuda, Thin Solid Films 445 (2003) 263.
[8] R. Janisch, P. Gopal, N.A. Spaldin, J. Phys, Condens. Matter 17 (2005) R657.
[9] Z. Jin, T. Fukumura, M. Kawasaki, K. Ando, H. Saito, Y.Z. Yoo, M. Murakami, Y. Matsumoto, T. Hasegawa, H. Koinuma, Appl. Phys. Lett. 78 (2001) 3824.
[10] H. Saeki, H. Tabata, T. Kawai, Solid State Commun. 120 (2001) 439.
[11] S. Suzuki, T. Miyata, M. Ishii, T. Minami, Thin Solid Films 434 (2003) 14.
[12] N.H. Hong, J. Sakai, A. Hassini, J. Appl. Phys. 97 (2005) 10D312.
[13] V. Avrutin, U. Ozgur, S. Chevtchenko, C. Litton, H. Morkoc, J. Electron. Mater. 36 (2007) 483.
[14] Y.C. Yang, C. Song, X.H. Wang, F. Zeng, F. Pan, Appl. Phys. Lett. 92 (2008) 012907.
[15] L. Wang, L. Meng, V. Teixeira, S. Song, Z. Xu, X. Xu, Thin Solid Films 517 (2009) 3721.
[16] K. Lovchinov, H. Nichev, O. Angelov, M.S. Vassileva, V. Mikli, D.D. Malinovska, J. Phys. Conf. Ser. 253 (2010) 012030.
[17] T. Matsuo, S. Okuda, K. Washio, Mater. Res. Soc. Proc. 1494 (2013), http://dx.doi.org/10.1557/opl.2013.157.
[18] H. Ushiki, Chemical Handbook, 5th ed. Maruzen, Tokyo, 2004. II-764.
[19] V.A. Ioffe, I.B. Patrina, Phys. Status Solidi 40 (1970) 389.
[20] S.A. Carter, J. Yang, T.F. Rosenbaum, J. Spalek, J.M. Honig, Phys. Rev. B 43 (1991) 1.